Experimental evaluation of different hydrodynamic modelling techniques applied to the ISWEC

Nicola Pozzi[#1], Andrea Castino[#2], Giacomo Vissio[#3], Biagio Passione[#4], Sergej Antonello Sirigu[#5], Giovanni Bracco[#6], Giuliana Mattiazzo[#7]

[#]*Department of Mechanical and Aerospace Engineering (DIMEAS), Politecnico di Torino*
C.so Duca degli Abruzzi, 14, 10129 Torino (TO), Italy

[1]nicola.pozzi@polito.it

[2]andrea.castino@polito.it

[3]giacomo.vissio@polito.it

[4]biagio.passione@polito.it

[5]sergej.sirigu@polito.it

[6]giovanni.bracco@polito.it

[7]giuliana.mattiazzo@polito.it

***Abstract*— The appropriate numerical modelling of a Wave Energy Converter behaviour is crucial for both the initial design phase (loadings estimations) and the productivity assessment of the real device, working in a certain installation site.**

The most difficult aspect to be modelled are the floater motions at resonance conditions, where motions amplitude are emphasised. Several techniques can be used, ranging from the linear Cummins' equation to fully viscous CFD simulations.

This paper deals with the implementation of the 3 DOFs linear hydrodynamic model developed for the time-domain simulation of ISWEC (Inertial Sea Wave Energy Converter) device. The main advantage of the model here presented is its low computational cost.

A first benchmarking between the numerical model and a series of tank testing experiments, carried out on a scaled ISWEC floater prototype, is described. Experimental results are used for the identification of the non-linearity due to the viscous effects. The novelty of the identification approach is the estimation of the non-linearity contribution along each DOF taken into account.

A second comparison is done against the open source code WEC-Sim that allows the calculation of the floater instantaneous wetted surface, with the aim of obtaining a cost-benefit evaluation of the different modelling techniques.

***Keywords*— Hydrodynamics modelling, Viscous forces, Tank Testing, Wave Energy, ISWEC.**

INTRODUCTION

The dynamics of a Wave Energy Converter (WEC) undergoing to the action of the waves is due to a combination of different typologies of external forces and moments (e.g. the forces due to the incident wave field, the radiation forces due to the floater motion, inertial forces, etc.).

Forces and moments distributions and the kinematic description of fluid motions are continuous in time and space, assuming that the collection of discrete fluid molecules can be analysed as a continuum [1].

The complex problem constituted by physical quantities distributed in time and space can be solved via Computational Fluid Dynamics (CFD) techniques. CFD numerical models constitutes the branch of high fidelity models, which allow to obtain an accurate description of the physical phenomena. On the other hand, the computational cost of CFD numerical models can be onerous. For this last reason they are not suitable for the WEC design and optimization, especially in the first stage, where the macroscopic physical parameters needs to be determined.

This complex problem is often simplified and described through lumped parameters models. The most recognized model that describes the dynamics of a floater is the well-known Cummins' equation [2]. The Cummins' equation is a linear differential equation with frequency dependent coefficients, widely used for the evaluation of the dynamics and hydrodynamic loadings on marine structures. In general, the hypothesis of linearity is fulfilled and the prediction given by the linear hydrodynamic equation is sufficiently reliable.

In the case of WECs, it is known that the power extraction is optimal when the device is in resonance conditions with respect to the frequency of the incoming wave [3]. In this operating condition, the motions amplitude can be very large, thus voiding the linearity hypothesis and therefore the WEC performances prediction.

In these conditions two kinds of non-linearity occur: the first one is related to the viscous effects induced by vortexes and to the intrinsic viscosity of the fluid; the second is due to the variation in time of the wetted surface. Both effects can be introduced in the linear model in order to improve its accuracy.

Viscous forces can be determined on the basis of CFD fully-viscous simulations or experimental wave tank testing [4][5], while the instantaneous wetted surface needs to be computed via specific numerical techniques [6].

In this work, a linear model based on the Cummins equation with constant mean wetted surface is considered. A series of experimental test performed on a scaled ISWEC floater prototype are used for the identification of the viscous forces. A detailed description of the identification

 Copyright © European Wave and Tidal Energy Conference 2017

methodology proposed is given. Then, viscous forces are introduced in the linear model in order to prove the better prediction of the floater dynamics in resonance conditions.

The validated numerical model is benchmarked with the WecSim open-source code that allows the computation of the instantaneous wetted surface [7]. The aim of the comparison is a cost-benefit evaluation of the different modelling techniques, since the computation of the instantaneous wetted surface leads to higher computational costs.

The cost-benefit analysis plays a role of considerable importance, in fact the main purpose of this work is to obtain a sufficiently fast and accurate hydrodynamic model that can be coupled with the conversion system, obtaining a complete tool for the WEC design and power matrix estimation [8].

LINEAR HYDRODYNAMIC MODEL

A. *Potential flow theory*

The linear hydrodynamic models are based on the linear potential flow theory, hold by the following hypotheses:

- The fluid flow is assumed inviscid, incompressible and irrotational;
- The incident wave is harmonic and regular;
- The incident wave acting on the body is characterized by small amplitude, when compared to its length;
- The body motions are sinusoidal and small with respect to the equilibrium position. Hence, the wetted surface is assumed constant in time;
- The body has zero or very small forward speed.

The theory defines a fluid flow field by means of a velocity potential that is composed by the sum of three components: radiation, incident and diffracted wave potentials [9].

The incident wave potential for a linear regular wave is known, while the remaining potentials need to be determined numerically. The panel method is the strategy commonly used in the potential flow codes available, such as Ansys AQWA, WAMIT or Nemoh. [9-11].

Once the potentials are known, then the pressure distribution over the wetted surface (supposed constant in time) can be derived starting from the linearized Bernoulli's equation.

The solution of the problem described above allows to determine the frequency dependent added mass and radiation damping coefficients, as well as Froude-Krylov and diffraction forces coefficients [9].

B. *Frequency-domain equation*

The results of the frequency domain analysis described in the previous paragraph can be used for the solution of the Cummins equation [2]. The general expression for the 6 Degrees of Freedom (DoFs) is given by the matrix equation (Eq. 1).

$$([M]+[A(\omega)])\{\ddot{X}\}+[B(\omega)]\{\dot{X}\}+[K]\{X\}=\{F_w(j\omega)\} \quad (1)$$

Where:

- $[M]$ represents the floater mass matrix;
- $[A(\omega)]$ is the frequency dependent added mass matrix;
- $[B(\omega)]$ corresponds to the frequency dependent radiation damping matrix;
- $[K]$ is the hydrostatic stiffness matrix;
- $\{F_w(j\omega)\}=\frac{H}{2}\{f_w(j\omega)\}$ is the wave force vector expressed as the product between the wave amplitude and the Froude-Krylov and diffraction coefficients per unit of wave amplitude;
- $\{X\}$ represents the six DoFs vector.

Starting from the frequency domain equation, it is possible to derive the Response Amplitude Operator (RAO), which represents the transfer function between the floater motion amplitude with respect to one of the six DoF and the wave amplitude. In (Eq. 2) the RAO expression for the *i-th* DoF (*i=1,2,..,6*) is given.

$$RAO=\frac{X_i}{\left(\frac{H}{2}\right)}=\frac{f_{w,i}(j\omega)}{-\omega^2(M_{ii}+A_{ii}(\omega))+j\omega B_{ii}(\omega)+K_{ii}} \quad (2)$$

In Fig. 1 an example of RAO is given for the pitch DoF. It is important to highlight that the frequency correspondent to the RAO peak represents the floater resonance frequency of the considered DoF.

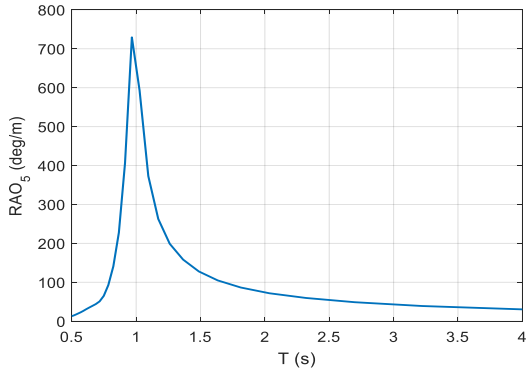

Fig. 1 Example of Response Amplitude Operator (RAO) evaluated for the pitch DoF of a floater

C. *Time-domain equation*

The six DoFs frequency-domain Cummins equation was converted into a time domain dynamic equation by Ogilvie in 1964. According to the Ogilvie's decomposition, (Eq. 1) becomes [12]:

$$([M]+[A(\infty)])\{\ddot{X}\}+\int_0^t[h_r(t-t')]\{\dot{X}\}dt'+[K]\{X\}=\{F_w(t)\} \quad (3)$$

Where $[A(\infty)]$ is the added mass matrix evaluated for infinite oscillation frequency, while $[h_r(t-t')]$ is the matrix of the impulse response function of the radiation forces. This function takes into account the fluid memory effect and incorporates the energy of the radiated waves generated by the motion of the body.

The numerical computation of the convolution integral is time consuming and for this reason not suitable for the design and analysis of WECs. Pérez and Fossen, in 2008, suggested a solution for the problem described above [13][14].

The methodology approximates the convolution integral with a Linear Time Invariant (LTI) parametric model in state-space form. Then the impulse response function is calculated through a parametric frequency-domain identification. The aim of the identification process is to find an appropriate order of the transfer function, which satisfies the criteria of minimum approximation error, stability and passivity. (Eq. 4) shows the approximation of the convolution integral with a LTI model, represented via state-space notation, for the *i-th* DoF.

$$F_{r,ij} = \int_0^t h_{r,ij}(t-t')\dot{X}_i dt' \cong \begin{cases} \dot{\zeta}_{r,ij} = A_{r,ij}\zeta_{r,ij} + B_{r,ij}\dot{X}_i \\ F_r = C_{r,ij}\zeta_{r,ij} + D_{r,ij}\dot{X}_i \end{cases} \quad (4)$$

It is important to highlight that (Eq. 1) involves only linear quantity in steady state conditions and it is valid only for monochromatic excitation forces. On the other hand, (Eq. 3) can be used also in the case of irregular wave forces and non-linear forces can be introduced, e.g. mooring forces, non-linear hydrodynamic forces, etc.

D. Non-linear viscous damping

As mentioned before, it is known that WECs performances are optimal when the device is in resonance with respect to the frequency of the incoming wave.

The resonance is a linear phenomenon, in which large motions amplitude of the structure can occur. On the other hand, in this condition the interaction between the floater and the fluid originates non-linear phenomena such as vortexes that damp the motions amplitude. Taking into account this aspect, it is clear that the linear hydrodynamic model does not predict accurately the floater dynamics in resonance conditions. The model can be improved introducing non-linear viscous corrections, increasing its accuracy and preserving the advantage of low computational costs, typical of the lumped parameters models.

In (Eq. 5) the expression of the viscous force for the *i-th* DoF is given. The non-linear term can be introduced in the time-domain equation (Eq. 3), as shown by (Eq. 6). The viscous coefficients can be determined through wave tank experimental tests or fully viscous CFD numerical simulations, based on the integration of the Navier-Stokes equations [4].

$$F_v = \beta_i \dot{X}_i \left|\dot{X}_i\right| \quad (5)$$

$$([M]+[A(\infty)])\{\ddot{X}\} + \int_0^t [h_r(t-t')]\{\dot{X}\}dt' + \{\beta\}\{\dot{X}\}\left|\{\dot{X}\}\right| + [K]\{X\} = \{F_w(t)\} \quad (6)$$

EXPERIMENTAL TANK TESTING

In this work, a methodology for the non-linear viscous damping identification is proposed, considering the case study constituted by ISWEC device. The parameters identification is obtained using experimental testing results carried out at the Hydrodynamic and Maritime Research Centre of the University College of Cork (HMRC) in 2015, on a scaled ISWEC floater prototype [15][16].

In this section, a brief overview of the ISWEC Wave Energy Converter is given, as well as a description of the scaled prototype and of the tank testing set up.

A. ISWEC device

ISWEC (Inertial Sea Wave Energy Converter) is an offshore floating device designed to exploit wave energy through the gyroscopic effects of a spinning flywheel.

In Fig. 2, a simplified scheme of the ISWEC device is reported. The system is composed by a sealed hull in which the gyroscopic unit, the Power Take Off (PTO) and all the subsystem required for the device functioning are enclosed. The device is kept in place through a slack mooring line connected from one side to the sea bed and to the other to the bow of the hull.

The action of the waves on the floater induces a pitching motion of the device. The gyroscope reacts with a precession motion that can be damped with a rotational PTO, allowing the energy extraction.

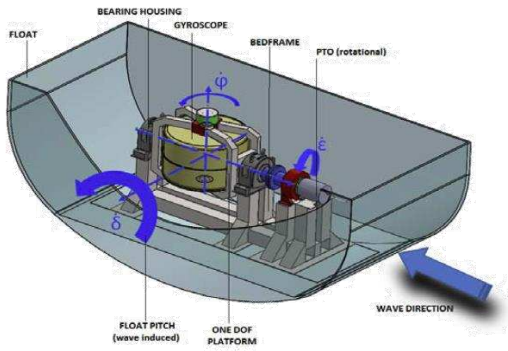

Fig. 2 Scheme of the ISWEC Wave Energy Converter

The main advantage of this technology is that all the mechanical components are sealed into the hull, thus avoiding the contact with the harsh sea environment, reducing the corrosion problems and maintenance costs. Furthermore the system, thanks to the specific shape of the floater and mooring line design, can self-align with respect to the incoming wave direction. Eventually, the flywheel speed can be tuned together with the PTO control parameters in order to increase the device performances in a wide range of wave conditions [17][18].

B. *Scaled prototype*

The scaled ISWEC floater prototype tested at HMRC wave basin was scaled referring to the full-scale device deployed in July 2014 in Pantelleria Island.

The scaling factor was determined considering both the range of the working condition of the full-scale plant, defined by the installation site scatter diagram represented in Fig. 3 and the capabilities of the HMRC wave basin [16][19].

In Table 1, the minimum and maximum significant wave height and energy period values are reported.

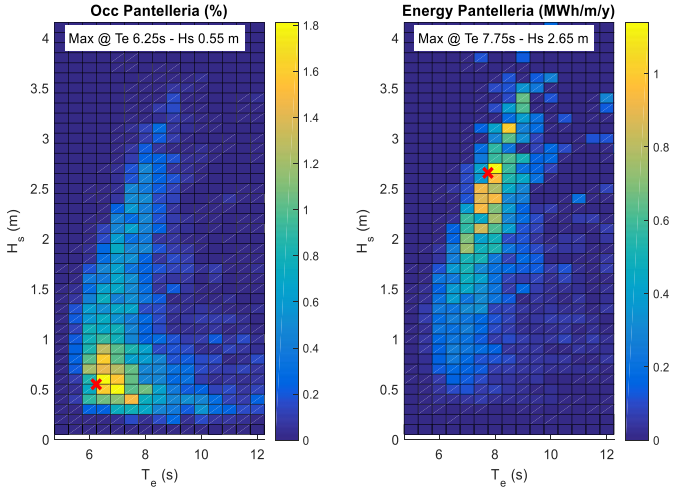

Fig. 3 Scatter diagram of the ISWEC installation site in Pantelleria Island

TABLE I
SIGNIFICANT WAVE HEIGHT AND ENERGY PERIOD RANGE

Parameter	ISWEC full scale	ISWEC 1:20	HMRC	Unit
$T_{e,min}$	5	1.1	0.6	s
$T_{e,max}$	10	2.2	2.5	s
$H_{s,max}$	3	0.15	0.18	m

According to the Froude scaling law [20], a 1:20 scale was determined. The ISWEC full scale properties were scaled down, in order to determine the features of the model. In Table 2, the main properties of the scaled floater are reported.

TABLE II
FLOATER PROPERTIES

Parameter	Scaling factor	ISWEC full-scale	ISWEC 1:20	Unit
Length	s^1	15	0.75	m
Width	s^1	8	0.4	m
Height	s^1	4.5	0.225	m
Mass	s^3	300e3	37.5	kg
Draft	s^1	3.18	0.159	m
Roll inertia	s^5	2.05e06	0.64	kgm^2
Pitch inertia	s^5	9.5e06	2.97	kgm^2
Yaw inertia	s^5	10.8e06	3.38	kgm^2
z_{COG}	s^1	-0.26	-0.013	m

The Froude scaling approach was used also for the estimation of the mooring line features. In Table 3, the features of the mooring line are reported.

TABLE III
MOORING LINE PROPERTIES

Parameter	Scaling factor	ISWEC full-scale	ISWEC 1:20	Unit
L_1	s^1	10	0.5	m
L_2	s^1	5	0.2	m
L_3	s^1	13	0.65	m
Mass	s^3	8000	1	kg
Jumper net buoyancy	s^3	12000	1.5	kg
Chain linear mass	s^2	45	0.113	kg/m

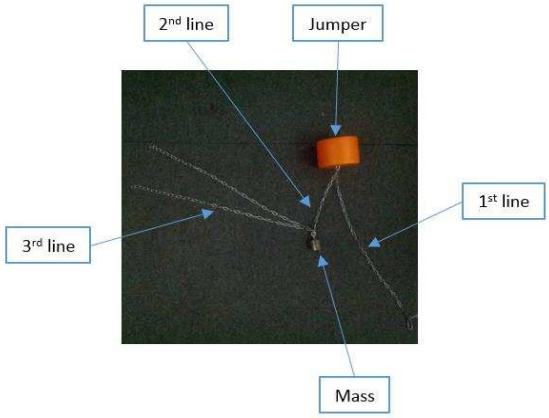

Fig. 4 ISWEC 1:20 mooring line

The compliant mooring system was built using a submerged jumper and a mass connected from one side to the seabed and to the other side to the hull, through three lines. Observing Fig. 4 it is possible to see that the third line is subdivided in two parts: one is connected to the left side of the floater and one to the other side, guaranteeing the possibility of self-alignment of the floater with respect to the incoming wave. The characteristics of this kind of mooring mimic a hardening spring behaviour, with reduced stiffness for small displacement and high restoring force at bigger displacements. Such behaviour allows small interactions with the floater for normal operations and high forces before end stroke, thus reducing snatches in extreme wave conditions.

C. *Experimental set up and moored system tests*

The prototype was moored 6.5 m far from the wave maker paddles, in the calibrated area defined by the capabilities of the motion tracking system, as shown in Fig. 5. In each edge of the calibrated area a wave probe was placed.

In Fig. 6, the moored device during the tank testing is depicted. On the deck of the device it is possible to individuate the reflecting markers used for the instantaneous tracking of the prototype motions along its 6 DoFs.

Taking into account the minimum and maximum values of the scaled wave properties and of the wave maker limits reported in Table 1, the following regular wave parameters were chosen (see Table 4).

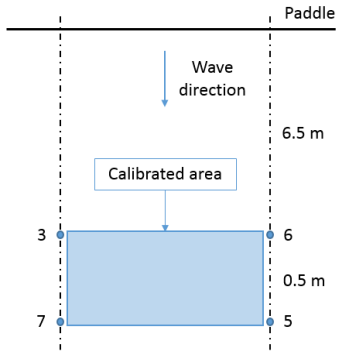

Fig. 5 Wave basin calibrated area and wave probes set up

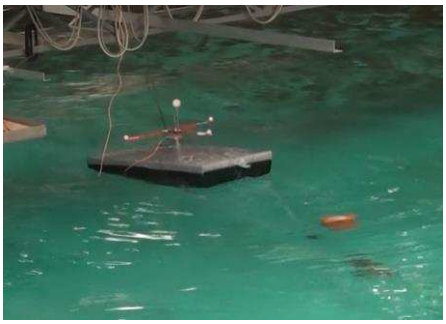

Fig. 6 ISWEC 1:20 moored in the wave basin during experimental activity

In Fig. 7, the RAO for heave and pitch DoFs experimentally determined for the two wave heights considered for this analysis, is depicted.

It is important to underline that heave RAO is not affected by the wave height, thus the linearity hypotheses are fulfilled. On the other hand, pitch RAO shows a dependency from wave height: this means that non-linear phenomena are involved.

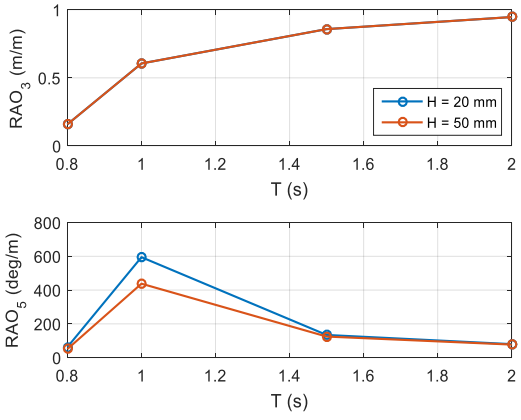

Fig. 7 Heave and pitch RAOs determined experimentally for the ISWEC 1:20 prototype.

TABLE IV
PARAMETERS OF THE REGULAR WAVE USED FOR THE TESTS

H (mm)	T (s)			
	0.8	**1**	**1.5**	**2**
20	x	x	x	x
50	x	x	x	x

NON-LINEAR VISCOUS DAMPING IDENTIFICATION

In this section, the methodology applied for the identification of the non-linear viscous damping is described, highlighting the assumptions and the most important features.

A. *Plane model*

The Cummins equation, as stated before, can be written for each one of the six DoFs.

As described previously, ISWEC is designed to be self-aligning with respect to the direction of the incoming wave. Thus, the plane problem constituted by surge, heave and pitch can be considered sufficient for the device dynamic representation.

The simulation of the WEC dynamics is performed in time-domain, where non-linear external forces, such as the viscous forces and mooring line forces can be included.

In particular, in the case of the plane model, viscous forces are introduced only for surge and pitch DoFs. Moreover the hydrodynamic problem needs to be completed by adding the drift force in the surge dynamic equation.

Regarding mooring forces, the third line is considered as a unique chain and the corresponding tension is decomposed along surge and heave directions. Since the connection point of the mooring line on the floater does not coincide with its centre of gravity, a torque component acting along the pitching axis needs to be added.

On the basis of the following assumptions, it is possible to write a set of three differential equations, as reported below.

$$\left(M_{11}+A_{11}(\infty)\right)\ddot{x}+F_{r,11}(t)+F_{r,15}(t)+\beta_{11}|\dot{x}|\dot{x}+K_{33}x= \\ =F_d(t)+F_{w,1}(t)+F_{m,1}(t) \tag{7}$$

$$\left(M_{33}+A_{33}(\infty)\right)\ddot{z}+F_{r,33}(t)+K_{33}z=F_{w,3}(t)+F_{m,3}(t) \tag{8}$$

$$\left(M_{55}+A_{55}(\infty)\right)\ddot{\delta}+F_{r,55}(t)+F_{r,51}(t)+\beta_{55}|\dot{\delta}|\dot{\delta}+K_{55}\delta= \\ =F_{w,5}(t)+F_{m,5}(t) \tag{9}$$

In (Eq. 7) and (Eq. 9) the off diagonal terms of the radiation forces matrix represent the couplings between surge and pitch DoFs.

B. *Numerical model*

The numerical model is realized in Matlab/Simulink® on the basis of (Eq. 7), (Eq. 8) and (Eq. 9) described in the previous section.

In Fig. 8, the block scheme of the Simulink model used for the floater dynamics representation is depicted.

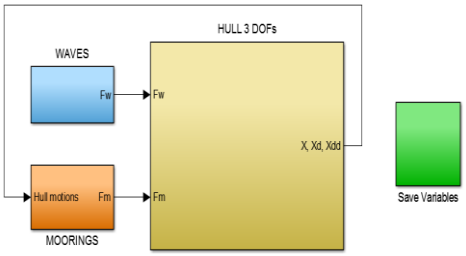

Fig. 8 Matlab/Simulink ® numerical model

The three main blocks are:

- *WAVES*: input block that contains the wave drift force along surge axis and the first order wave forces (Froude-Krylov and diffraction forces) along the three DoFs;
- *HULL*: in this block the time-domain Cummins equation for each DoF is implemented according to (Eq. 7), (Eq. 8) and (Eq.9). The corresponding hydrodynamic coefficients are determined by using Ansys AQWA. Here the couplings between surge and pitch motion are also present together with the non-linear viscous forces. It is important to notice that the radiation forces are modelled via state space representation as described by (Eq. 4). The outputs of this block are the hull motions, velocities and accelerations along surge, heave and pitch directions;
- *MOORINGS*: mooring line forces are described through a quasi-static representation. In this block mooring forces are computed by means of a Look-Up Tables (LUTs), containing the relation displacement-force of the mooring line. LUTs are computed off-line.

C. Identification methodology

1) Wave forces determination: The wave forces are determined considering the real wave elevation measured in the wave basin. As shown by Fig. 9, the regular wave profile may differ from the theoretical one, assumed to be an ideal sinusoidal function.

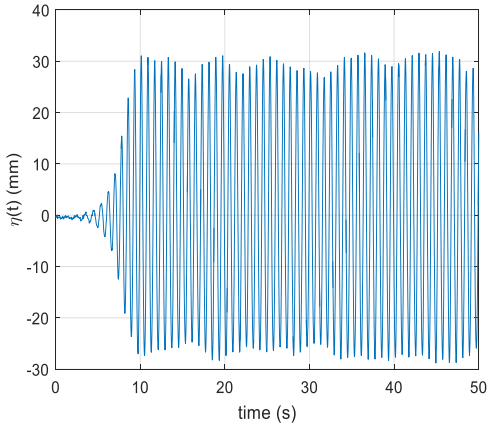

Fig. 9 Experimental wave profile at H=50 mm and T = 1s

A Fast Fourier Transform (FFT) can be performed in order to determine the wave spectrum that combined with the frequency dependent Froude-Krylov and diffraction forces coefficients allows to build the wave forces time series as the superimposition of all monochromatic contributions (see Eq. 10).

$$F_w(t) = \sum_{n=1}^{N} F_{w0,n} \cos(\omega_n t + \phi_n + \vartheta_n) \tag{10}$$

Where:

- $F_{wo,n} = \sqrt{2|f_w(j\omega_n)|^2 S_\eta(\omega_n)\Delta\omega}$ is the amplitude of the *n-th* force component. Note that the amplitude of the force component depends on the one-sided wave spectrum $S_\eta(\omega)$;
- $\phi_n = \angle(f_w(j\omega_n))$ is the phase due to the Froude-Krylov and diffraction coefficients;
- ϑ_n is the phase between the harmonic components of the spectrum $S_\eta(\omega)$.

A similar approach is adopted for the wave drift forces. In this work the time-domain drift force was determined by using the Newman's approximation [21], given by Eq. 11.

$$F_d(t) = 2\left(\sum_{n=1}^{N} \sqrt{2 f_d(\omega_n) S_\eta(\omega_n)\Delta\omega}\cos(\omega_n t + \vartheta_n)\right)^2 \tag{11}$$

$f_d(\omega)$ correspond to the drift force coefficients determined through the potential flow code (Ansys AQWA).

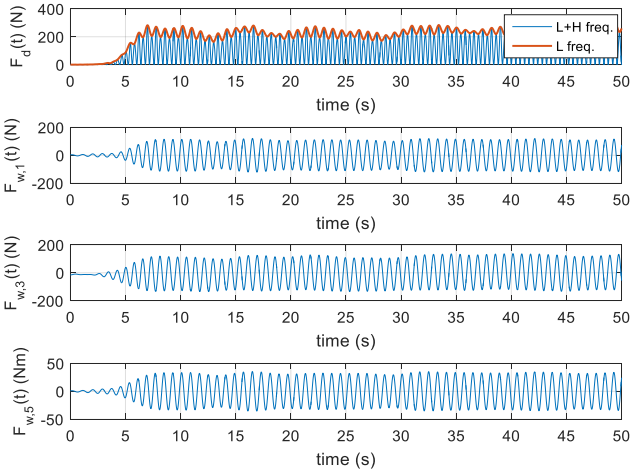

Fig. 10 Wave forces along surge, heave and pitch DoFs, generated from the experimental wave profile at H=50 mm and T=1 s

Newman's approximation allows to reduce the computational costs for the determination of the time-domain drift force when the complete Quadratic Transfer Functions

(QTFs) are used. For the sake of brevity, the complete justification about the Newman's approximation is here omitted and more details can be found in [22].

In Fig.10 an example of the calculated time-domain wave forces is depicted for the different DoF.

2) Numerical simulation: The wave forces time series determined at the previous step constitutes the input for the numerical model of the floater. In this step the time domain floater motions are computed.

3) Time series FFT analysis: The numerical and experimental motion time series are analysed by means of the FFT, in order to determine the amplitude and the frequency of the motions. Before the application of the FFT algorithm, a proper interval of the time series is selected with the aim to exclude the initial transient, then the mean value is removed and the signal is cut over an integer number of cycles. In Fig. 11, an example of the results of the FFT analysis performed over the experimental data is represented. The dashed line corresponds to the amplitude calculated through the FFT analysis. In the case of the surge motion the amplitude coincides with the first peak. In fact, as it is explained in the next paragraph, only the amplitude of the first peak with respect to the steady state position is used for the non-linear hydrodynamic forces identification.

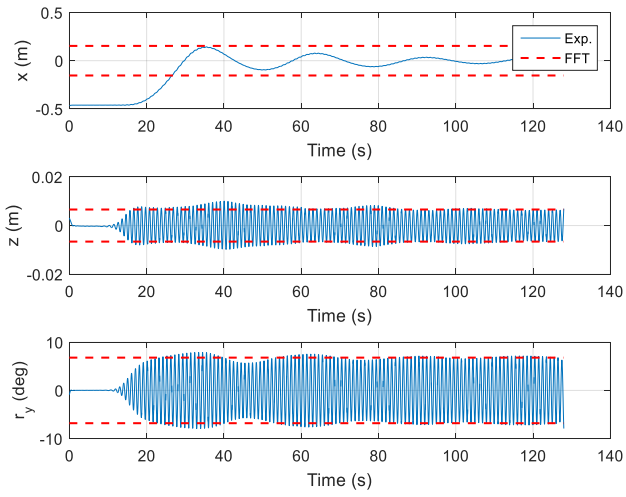

Fig. 11 Example of the FFT analysis results performed over the floater motion experimental data

4) Non-linear viscous damping identification: The amplitude of the numerical and experimental time series obtained from the FFT analysis are compared. An optimization algorithm, the Nelder-Mead simplex algorithm [23], is used in order to identify the non-linear viscous damping coefficients that minimizes the differences between the two datasets. At this stage, the numerical model is run recursively until the objective of the optimization procedure is reached. It is important to highlight that at the end of each run the FFT analysis over the numerical data is performed, according to the criteria given in the previous paragraph.

NUMERICAL MODEL VALIDATION

The methodology described in previous section, was applied considering the regular wave condition corresponding to the floater resonance wave period. As described previously, the aim of this analysis is to verify also the dependency of the viscous forces with respect to the wave amplitude. Table 5 summarizes, the results carried out from the identification procedure for surge and pitch DoFs.

TABLE V
RESULTS OF VISCOUS DAMPING COEFFICIENT IDENTIFICATION

H (mm)	T (s) = 1s	
	Surge (Nms^2/m^2)	Pitch (Nms^2/rad^2)
20	50.11	0.588
50	57.64	0.695

Observing Table 5, it is possible to see that both coefficients shows a dependency with the wave amplitude. In particular, doubling the wave height, the viscous coefficients increases around 15%.

The viscous coefficients previously determined are introduced in the numerical model and the correspondence between numerical and experimental data is checked for each one of the DoFs taken into account.

A. Surge DoF

The surge motion, as described previously, is excited by two different kind of wave forces: the Froude-Krylov and diffraction and drift forces. In this case, it is not possible to determine the RAO. For this reason a comparison of the time series is presented.

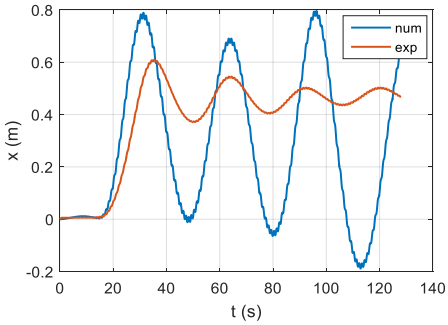

Fig. 12 Surge motion at H = 50 mm and T = 1, without non-linear viscous damping

In Fig. 12, the response of the system along surge DoF when excited with a 50 mm wave amplitude and 1 s wave period is shown. The horizontal viscous force is here neglected: the surge motion amplitude is very large and the predicted behaviour is not representative of the real system.

Introducing the non-linear viscous damping a better representation of the phenomena is achieved, even if the steady state position is not well described, as shown in Fig. 13.

A not completely successful prediction for the steady state condition is revealed also at longer wave period, as represented in Fig. 14.

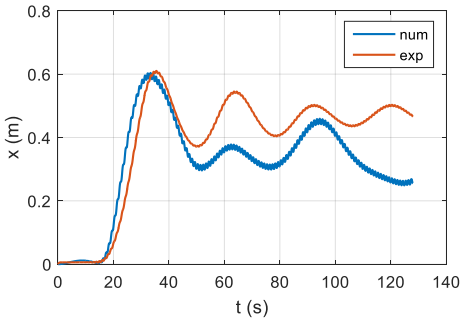

Fig. 13 Surge motion at H = 50 mm and T = 1 s, with non-linear viscous damping

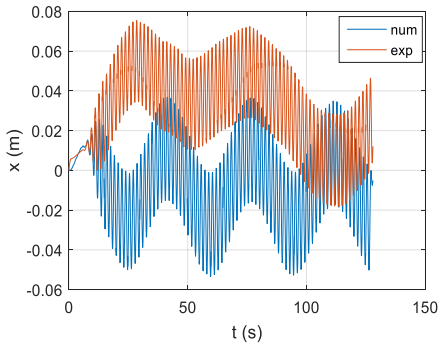

Fig. 14 Surge motion at H = 50 mm, T = 1.5 s, with non-linear viscous damping

In order to better understand such difference, in Fig 15, the numerical and experimental steady state values normalized with respect to the wave amplitude are plotted against the respective wave period.

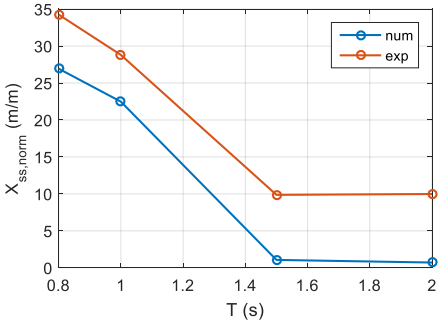

Fig. 15 Numerical and experimental surge steady state position, normalized with respect to the wave amplitude

The trend of the numerical model is in agreement with experimental data: the steady state position value decreases with the increasing of the wave period, since drift force decreases with the wave period. On the other hand, the difference between experimental and numerical data may be explained taking into account the following causes: the first regards the absence of the mooring line dynamic effects, while the second is related to the fact that drag forces are neglected. It is important to underline that the effect of these forces becomes important when the wave period increases [22].

B. Heave and Pitch DoF

The heave and pitch DoFs can be validated by comparing the corresponding RAOs, determined numerically and experimentally. The comparison is performed taking into account also the effect of non-linear viscous forces on pitch DoF.

In Fig. 16 and in Fig. 17, the results obtained in the case of the 20 and 50 mm wave height are represented, respectively.

In both cases, it is possible to highlight the satisfactory correspondence between the numerical and experimental data for the heave DoF.

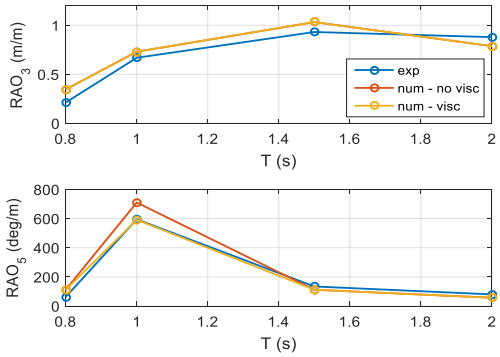

Fig. 16 Numerical and experimental heave RAO (top) and pitch RAO (bottom) for the 20 mm wave height tests

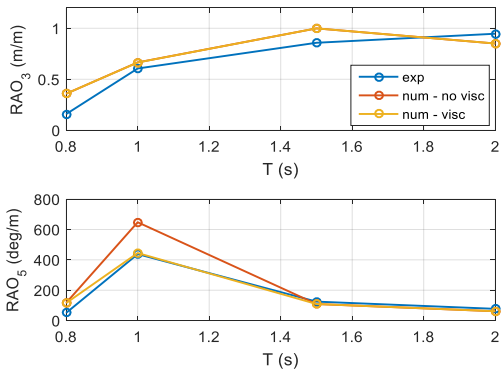

Fig. 17 Numerical and experimental heave RAO (top) and pitch RAO (bottom) for the 50 mm wave height tests

Regarding the pitch DoF, it is possible to see the remarkable difference of motion amplitude in resonance condition and in particular, as described previously, the effect of the non-linearity is greater in the case of higher wave amplitude. Introducing the non-linear viscous effects, a better prediction of the motion can be achieved.

It is important to remark that the pitch RAOs with viscous effects are determined considering the constant value calculated through the optimization procedure, for all the wave period considered, i.e. the identified viscous damping coefficient is frequency independent.

In Fig. 18 an example of time series corresponding to the test with 50 mm wave amplitude and 1 s wave period is reported, proving the satisfactory prediction of the floater motions.

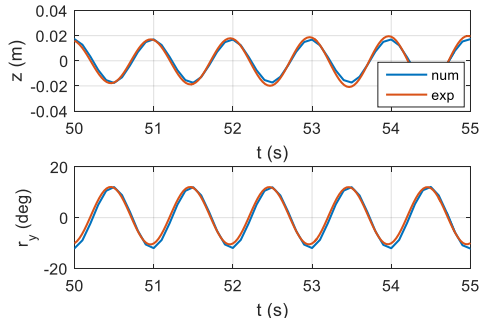

Fig. 18 Numerical and experimental heave and pitch motions determined at H = 50 mm, T = 1 s, with viscous damping

WEC-SIM BENCHMARKING

In this section, the numerical model previously developed and validated is benchmarked with the Wec-Sim open-source code, developed specifically for the WECs simulation. In Fig. 19, the SimMechanics model built using the Wec-Sim library is shown.

The analysis here proposed is a first attempt for the comparison between two different numerical modelling techniques, in terms of motion prediction accuracy and computational cost. The aim is to determine the most convenient technique to be used for the time-domain simulation of the system.

It is important to underline that the Wec-Sim tool, allows to perform the time-domain simulation according to different modalities: the first one corresponds to the solution of the fully linear problem with mean wetted surface (Cummins equations), while the second introduces the computation of the instantaneous wetted surface, thus the non-linear Froude-Krylov forces and the non-linear hydrostatic stiffness.

Those effects are mainly related to a geometrical non-linearity that, as the viscous forces, become important when the floating structure reaches its resonance frequency.

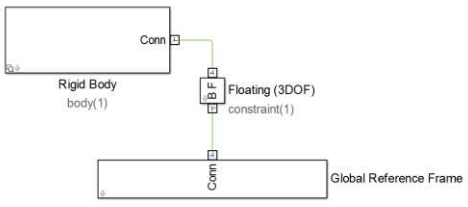

Fig. 19 Floater SimMechanics model, built using the Wec-Sim library

Despite the computation of the instantaneous wetted surface allows to increase the accuracy of the floater hydrodynamic representation, the identification of the viscous forces is still required. Moreover, the calculation of the instantaneous wetted surface results in a higher computational cost.

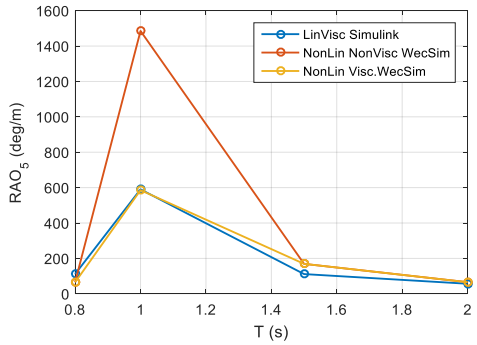

Fig. 20 Pitch RAO comparison at H = 20 mm

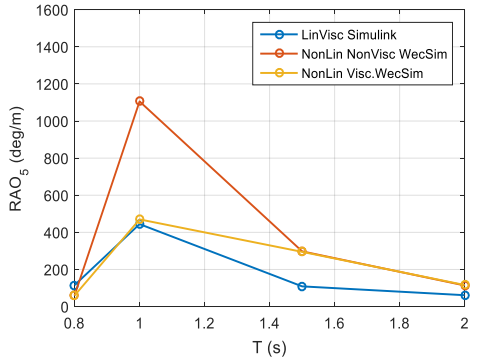

Fig. 21 Pitch RAO comparison at H = 50 mm

Fig. 20 and Fig. 21 show, respectively, the comparison between the pitch RAO computed with the Simulink linear model improved with viscous forces and with the Wec-Sim model with the calculation of the instantaneous wetted surface, for the two different experimental wave heights.

For a sake of simplicity only the pitch DoF is investigated. Wec-Sim simulations performed without non-linear viscous forces lead to the overestimation of the floater pitching motion in correspondence of the resonance period. The same result is achieved with the simpler model based on the mean wetted surface. Also in the case of the Wec-Sim simulation, the non-linear viscous coefficient has been identified, obtaining a satisfactory prediction of the pitch motion amplitude.

Apparently there is no difference between the two modelling techniques, despite a proper identification of the non-linear viscous coefficients on the basis of experimental data. However, it is important to highlight that the computational cost of the instantaneous wetted surface Wec-Sim model is higher than the mean wetted surface Simulink model. For instance, considering 100 s of regular sea state, the mean wetted surface model takes less than 1 s, while the Wec-Sim model takes around 20 s.

On the other hand, as suggested by Penãlba [24], the non-linear Froude-Krylov forces modelling becomes relevant when the PTO control law is considered.

CONCLUSIONS

This paper deals with the implementation of the 3 DoFs ISWEC hydrodynamic model, based on the linear Cummins equation.

It is well known that the WECs power extraction is optimal when the device resonance frequency matches with the incoming wave frequency. In resonance conditions, different non-linear effects occur: for this reason the linear hydrodynamic model does not allow a reliable prediction of the floater motions.

The numerical model proposed is improved introducing the effect of non-linear viscous forces on surge and pitch DoFs, where the influence of such forces is greater. The non-linearity are identified on the base of experimental data carried out at HMRC wave basin in Cork, on a scaled ISWEC floater prototype. The results of the identification show a slight dependency of non-linear viscous coefficients with respect to the wave amplitude. However, from the practical point of view, it is possible to determine an average value, which is necessary when the irregular sea state is considered.

The 3 DoFs linear model previously developed is then benchmarked with the Wec-Sim code that allows to distinguish the geometrical non-linearity due to the instantaneous wetted surface (non-linear hydrostatic stiffness and non-linear Froude-Krylov forces) and the non-linearity related to the viscous forces.

The comparison between linear and Wec-Sim models shows that there is not a sensible difference in terms of motion prediction once the viscous non-linearity are introduced properly. Actually, the unique difference is represented by the increasing of the computational cost due to the calculation of the instantaneous wetted surface at each time step. However, as suggested by different authors, the effect of non-linear Froude-Krylov forces can be relevant when the PTO control system coupled with the hydrodynamic model [24].

At this stage the linear model proposed can be considered a good representation of the ISWEC floater dynamics, with the benefit of relatively low computational costs.

Future activity will regard the coupling of the hydrodynamic models analysed in this work with the gyroscope dynamic model and the investigation of their accuracy. In particular, the influence of non-linear wave excitation forces on the performances prediction will be evaluated.

ACKNOWLEDGMENT

The access to the HMRC tank infrastructure was financed in the framework of the EU project FP7-Infrastructues 262552 / MaRINET “Marine Renewables Infrastructure Network for Emerging Energy Technologies”.

REFERENCES

[1] J. M. Journée and W. W. Massie, *Offshore Hydromechanics*, 1st ed., Delft University of Technology, 2001.

[2] W. E Cummins, “The impulse response function and ship motion,” David Taylor model basin, Department of the Navy, Washington DC, Tech. Rep. 1661, 1962.

[3] J. Falnes, *Ocean Waves and Oscillating Systems: Linear Interaction Including Wave-Energy Extraction*, 1st ed., Cambridge University Press, 2002.

[4] R. M. Penãlba, G. Giorgi and J. Ringwood, “A review of nonlinear approaches for wave energy modeling,” in *Proc. 11th EWTEC Conference*, 2015, ISSN 2309-1983.

[5] M. A. Bhinder, A. Babarit, L. Gentaz and P. Ferrant, “Assesment of Viscous damping via 3D-CFD Modelling of a Floating Wave Energy Device,” in *Proc. 9th EWTEC Conference*, 2011.

[6] S. X. Du, D. A. Hudson, W.G. Price and P. Temarel, “Implicit expressions of static and incident wave pressures over the instantaneous wetted surface of ships,” Fluid-Structure Interactions: special issue in honor of Professor W. Geraint Price Proceedings of the Institution of Mechanical Engineers, *Journal of Engineering for the Maritime Environment*, vol. 223, no. 3, pp. 239-256.

[7] (2017) The Wec-Sim website. [Online]. Available: https://wec-sim.github.io/WEC-Sim/

[8] G. Bracco, E. Giorcelli, G. Giorgi, G. Mattiazzo, B. Passione, M. Raffero and G. Vissio, “Performance Assessment Of The Full Scale Iswec System,” in *Proc. ICIT 2015*, Sevilla, 17-19 March 2015, pp. 2499-2505.

[9] “AQWA Theory Manual, Release 15.0”, USA.

[10] “WAMIT User Manual, 2015”, USA.

[11] (2017) The Nemoh website. [Online]. Available: https://lheea.ec-nantes.fr/logiciels-et-brevets/nemoh-presentation-192863.kjsp

[12] T. F. Ogilvie, “Recent progress towards the understanding and prediction of ship motion,” in *Proc. Fifth Symposium of Naval Hydrodynamics*, 1964, Bergen, Norway, ACR-112, pp. 3-79, ONR.

[13] T. Perez and T.I. Fossen, “Time- vs. frequency-domain identification of parametric radiation force models for marine structure at zero speed,” *Identification and Control: A Norwegian Research Bulletin*, vol. 29, pp. 1-19, 2008.

[14] T. Perez and T.I. Fossen, “A matlab toolbox for parametric identification of radiation-force models of ship and offshore structures,” *Identification and Control: A Norwegian Research Bulletin*, vol. 30, pp. 1-15, 2009.

[15] (2017) The HMRC. [Online]. Available: https://www.ucc.ie/en/hmrc/.

[16] M. Raffero, G. Bracco, B. Passione, G. Vissio, G.Mattiazzo and E. Giorcelli, “Identification of the hydrodynamic parameters of a wave energy converter,” in *Proc. 11th EWTEC Conference*, 2015.

[17] S. A. Sirigu, G. Vissio, G. Bracco, E. Giorcelli,B. Passione, M. Raffero and G. Mattiazzo, “ISWEC design tool,” *International Journal of Marine Energy*, vol. 15, pp. 201-213, Sep 2016.

[18] G. Vissio, D. Valério, G. Bracco, P. Beirão, N. Pozzi and G. Mattiazzo, “ISWEC linear quadratic regulator oscillating control,” *Renewable Energy*, vol. 103, pp. 372-382, Apr 2017.

[19] N. Pozzi, G. Bracco, B. Passione, S. A. Sirigu, G. Vissio and G. Mattiazzo, “Wave Tank Testing of a Pendulum Wave Energy Converter 1:12 Scale Model,” *International Journal of Applied Mechanics*, vol. 9, no. 2, Mar 2017.

[20] T. McCombes, C. Johnstone, B. Holmes, L. E. Myers, A. S. Bahaj, V.Heller, J. P. Kofoed, J. Finn and C. Bittencourt, “Deliverable 3.3 Assessment of current practice for tank testing of small marine energy,” Equimar, Commission of the European Communities, 2010.

[21] J. N. Newman, “Second-order, slow-varying forces on vessels in irregular waves”, in *Proc. International Symposium Dynamics of Marine Vehicles and Structure in Waves*, Ed. Bishop RED and Price WG, Mech. Eng. Publications Ltd, London, 1974.

[22] O. M. Faltinsen, *Sea Loads On Ship and Offshore Structures*, 1st ed., Ocean Technology Series, Cambridge University Press, 1990.

[23] J. C. Lagarias, J. A. Reeds, M. H. Wright, and P. E. Wright, "Convergence Properties of the Nelder-Mead Simplex Method in Low Dimensions," *Journal of Optimization*, vol. 9, no. 1, pp. 112-147, 1998.

[24] R. M. Penãlba, A. Mérigaud, J. Gilloteaux and J. Ringwood, “Nonlinear Froude-Krylov force modelling for two heaving wave energy point absorbers,” in *Proc. 11th EWTEC Conference*, 2015.